



Ultrasonication-assisted Synthesis of High Aspect Ratio Gold Nanowires on Graphene Template and Investigation of Their Growth Mechanism

Journal:	<i>ChemComm</i>
Manuscript ID	CC-COM-03-2018-001727
Article Type:	Communication

SCHOLARONE™
Manuscripts



Journal Name

COMMUNICATION

Ultrasonication-assisted Synthesis of High Aspect Ratio Gold Nanowires on Graphene Template and Investigation of Their Growth Mechanism

Received 00th January 20xx,
Accepted 00th January 20xx

DOI: 10.1039/x0xx00000x

www.rsc.org/

Wenbo Xin,^{a*} Igor M. De Rosa,^{a,b} Yang Cao,^c Xunqian Yin,^d Hang Yu,^a Peiyi Ye,^a Larry Carlson^b and Jenn-Ming Yang^a

We report a facile synthesis of Au nanowires (AuNWs) with high aspect ratio (l/D) up to 5,000 on plasma activated graphene template with ultrasound assistance. We demonstrate that ultrasonication induced symmetry breaking of Au clusters facilitates the growth of AuNWs from embryonic stages. Furthermore, the growth mechanism of AuNWs is systematically investigated using high resolution electron transmission microscopy (HRTEM), which reveals the unique role of defective graphene template in directing the growth of AuNWs.

Graphene, serving as a versatile template for constructing novel nanocomposites, has aroused increasing interests recently.¹ Foreign materials built on graphene (G)/ graphene oxide (GO) templates include but not limited to noble metals,^{2,3} metal oxides,⁴ and organic crystals⁵ for a variety of emerging applications. Of particular interest are dimension- and structure-tunable Au nanocrystals assembled on the graphitic substrates, since such assemblies demonstrate multi-functional performances in innovative areas.⁶⁻⁸ Despite many kinds of anisotropic Au nanocrystals⁹⁻¹¹ were successfully grown on G/GO supports directly, there has been relatively little attention paid to the growth of one-dimensional Au nanowires (1-D AuNWs) on graphene template, particularly with high aspect ratios, i.e. length (l)/diameter(D). As an alternative of 1-D nanostructure, Au nanorods integrated with G/GO are extensively investigated.^{8,12-14} However, the obvious limitation of Au nanorods is their aspect ratio, which is normally less than

50.¹² Moreover, the mechanism of graphene directed growth of 1-D Au nanorods/nanowires remains so far elusive.

Symmetry breaking has been recently discovered as an imperative moment that precedes the anisotropic growth of nanocrystals.^{15,16} To trigger such an event, a variety of experimental strategies are applicable, such as asymmetric passivation, oxidative etching, lattice mismatch, etc.^{17,18} Accordingly, the most common approach to synthesize anisotropic Au nanocrystals employs additives serving as capping agents, such as Ag⁺ and halide ions.¹⁹⁻²¹ Up to date, however, there have been few reports on the external force, i.e. ultrasound induced symmetry breaking of Au clusters coupled with the graphene templates.

Here we demonstrate a facile synthesis of AuNWs with aspect ratios up to 5,000 on plasma activated graphene multilayers with the aid of ultrasonication. To the best of our knowledge, this is the highest aspect ratio of AuNWs ever synthesized directly on the graphene template. We have systematically investigated the growth of AuNWs from the nucleation stage to the growth completion, showing both ultrasonication induced symmetry breaking as well as the induction from graphene template are of critically importance in obtaining such AuNWs.

The synthesis is based on a spontaneous redox reaction between gold precursor (Au³⁺) and -sp² carbon network of graphene multilayers. Electrons transfer can be identified from the Raman spectroscopy (Fig. S1). Plasma treatment effectively oxidized the sp² carbon network, leading to the enhanced I_D/I_G in Raman spectrum. When Au⁰ was reduced from gold precursor (Au³⁺), graphene was further oxidized and gave rise to even larger I_D/I_G. The redshift of G peaks (inset of Fig. S1), usually caused by the doping activity, is a sign of the electrons transfer.²² As a consequence, AuNWs are dispersed sparsely on plasma activated graphene multilayers (Fig. 1(a)). Two ends of a typical nanowire are annotated with red arrows. With a higher magnification image (Fig. 1(b)), the length (l) of the nanowire is estimated as 55 μm, whereas its diameter (D) is ~15 nm (Figs. 1(c) and (d)), resulting in an aspect ratio, i.e. $R = l/D$, ≈ 3,667. From their diameter and length distributions shown in Figs.

^a Department of Materials Science and Engineering, University of California, Los Angeles, 410 Westwood Plaza, Los Angeles, California 90095 USA. Email: kevin.xwsu@gmail.com

^b Institute for Technology Advancement, University of California, Los Angeles, 410 Westwood Plaza, Los Angeles, California 90095 USA

^c Atmospheric Data Solutions, LLC., 1992 Racquet Hill, Santa Ana, California 92705 USA

^d School of Materials Science and Engineering, Shandong University of Science and Technology, 579 Qianwangang Rd., Economic & Technological Development Zones, Qingdao, Shandong 26650 China

Electronic Supplementary Information (ESI) available: [details of any supplementary information available should be included here]. See DOI: 10.1039/x0xx00000x

S2(a) and (b), the average R is $\sim 4, 200$. In addition, the largest R obtained is up to 5,000, confirmed by a nanowire with a length of 100 μm and a diameter of 20 nm, as shown in Figs. S3(a) and (b). More representative SEM images of G/AuNWs assembly can be found in Figs. S3(c) and (d).

On the other hand, the average R of AuNWs synthesized without ultrasound is significantly lower ($\sim 1, 100$), as shown in Figs. S2(c) and (d), mainly due to larger average diameters with a wide range from 20 nm to more than 100 nm (Fig. S4). This result suggests a key function of ultrasonication in inducing more uniform and high-aspect ratio AuNWs on graphene template.

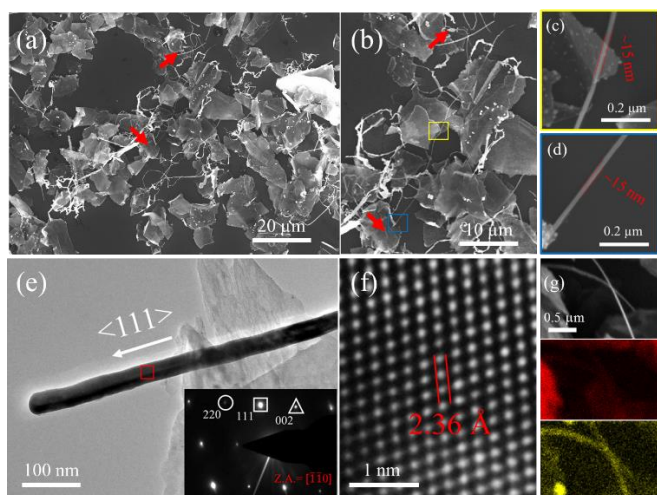


Figure 1. (a) A representative SEM image of the G/AuNWs nanocomposite. (b) Enlarged image of a selected area in (a). High-magnification images of the nanowire section highlighted in the yellow box (c) and blue box (d). (e) A typical TEM image of a single AuNW and its electron diffraction pattern. (f) Atomic structure of the area highlighted in the red box in (e). (g) Elemental mapping of G/AuNWs. Carbon element is shown in red, while gold is in yellow.

Moreover, Fig. 1(e) shows a representative TEM image of a single Au nanowire. The inset is its selected-area electron diffraction (SAED) pattern, which demonstrates a typical face-centred cubic (FCC) single-crystalline structure with $[\bar{1}10]$ as the zone axis. From the atomic structure of its selected area, we measured a lattice distance of $\sim 2.36 \text{ \AA}$ (Fig. 1(f)), consistent with the interplanar distance of Au $\{111\}$. This also confirms the growth direction of AuNWs is along $\langle 111 \rangle$, as indicated in Fig. 1(e). Meanwhile, FCC crystalline structure of AuNWs can be identified by X-ray powder diffraction (XRD) (Fig. S5). In contrast to polycrystalline Au whose texture coefficient (TC) of $\{220\}$ peak is 0.29, TC of AuNWs obtained here reaches to 1.21. (See Table S1 for details). Considering all of observed AuNWs grow along in-plane directions of graphene template, i.e. parallel to the graphene surface, we can justify AuNWs, or a majority of AuNWs obtained here are $\{220\}$ -orientated single-crystalline nanocrystals. In addition, elemental analysis shown in Figs. 1(g) illustrates the nanowires are pure gold, since only C and Au without any other elements are detected (Fig. S6).

We attribute the increased aspect ratio to the employment of ultrasonication as the external shear force that breaks Au clusters' symmetry at early stages and facilitates the attachment of Au clusters. Fig. 2 presents morphological differences of Au clusters formed on graphene template during

the nucleation stage ($\sim 30 \text{ min}$) with and without ultrasound usage.

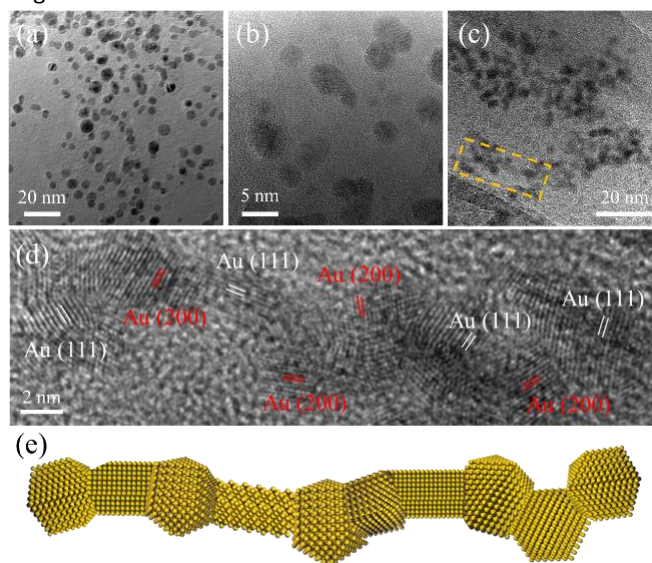


Figure 2. Symmetry breaking of gold clusters with the aid of ultrasound. Low (a) and high (b) magnification of TEM images of Au clusters grown on graphene template without ultrasound assistance. (c) A representative TEM image of Au clusters synthesized on graphene using ultrasonication. (d) Higher magnification image of the selected area in the dotted box in (c). (e) Schematic illustration of the atomic structure of the Au nanowire in (d).

On one hand, Au clusters obtained without ultrasonication mostly display as monodispersed spherical nanoparticles at this stage (Fig. 2(a)). Despite a few nanoparticles occasionally show coalescence, it barely extends to a continuous nanowire (Fig. 2(b)). On the other hand, Au clusters are observed to be attached and aligned to form an ultrathin nanowire ($D \sim 2 \text{ nm}$) with ultrasound (Fig. S7 and Fig. 2(c)). The corresponding FFT in Fig. S7(b) reveals Au nanocrystals with strikingly intense reflections from Au $\{111\}$ and $\{200\}$ planes, suggesting oriented Au clusters rather than randomly distributed ones nucleated on the defective graphene template. Furthermore, their atomic structure clearly justifies the selected section is composed of alternating Au $\{111\}$ and Au $\{200\}$ domains (Fig. 2(d)). Such an interesting structure can be elaborated from its schematic illustration in Fig. 2(e). The attachment of oriented nanoparticles is recognized as one of the potential options to realize the symmetry breaking.¹⁷

Moreover, this result suggests the ultrathin Au nanowire is formed via oriented-attachment (OA) process with the characteristic of sharing a common crystallographic plane, which has been widely reported as the growth mechanism of many anisotropic nanocrystals.²³⁻²⁵ In this study, symmetry breaking of Au clusters is triggered more rapidly with high shear force from the ultrasonication compared with those without it. In the latter case, Au nanoparticles can only coalesce when reach to bigger sizes, resulting in AuNWs with larger diameters and shorter lengths, as shown in Figs. S2 and Figure S4.

Remarkably, metal or metal oxide-ligand (substrate) interactions is of importance in determining the structures as well as properties of the assembly.²⁶⁻²⁸ It has been reported AuNWs synthesized from hydrothermal reactions using template-free and soft-template strategies are mostly

polycrystalline associating with wavy and branched shapes.²⁹⁻³² Meanwhile, we have noted a fair number of reports presenting the success in the synthesis of ultrathin AuNWs,^{25,33-36} including those coupled with graphitic substrates, such as GO and carbon nanotubes;^{35,36} However, shaping surfactants, such as oleylamine and cetyltrimethylammonium bromide (CTAB) were imperatively included in these studies. Here, surfactant-free synthesized AuNWs on graphene template strongly imply such a template plays a critical role.

In order to explore the explicit growth mechanism of AuNWs on the graphene, we devised a series of experiments in different timeframes and recorded their structural evolution step by step using HRTEM. The representative four steps were selected, i.e. 1 hr, 4 hrs, 12 hrs and 24 hrs, as shown in Fig. 3. At 1 hr, ultrathin Au nanowires with alternating orientations are modified to the ones with multiple twinned Au {111} structure (Fig. 3(a)), presenting the tendency to become single-crystalline. Such a modification is likely derived from a 3-D rotation of Au clusters, in order to align different crystallographic planes on graphene surfaces, which indicates relatively weak bonding between Au clusters and graphene template during the growth. As reported, interfaces elimination via 3-D rotation is one of the pathways to fulfil OA process.^{37,38} With time going on, we observe AuNWs associated with neck-like characteristic, which is another indication of OA. The connection between different Au sections causes concave parts along the nanowire (as pointed by the red arrow in Fig. 3(b)), which serve as "hotspots" for fresh Au nanoparticles to preferentially attach driven by localized Ostwald ripening.³⁸ Noticeably, AuNWs at this stage mainly elongate longitudinally with a favourable direction, instead of growing along multiple directions that would ultimately form branched shapes. This mainly benefits from the graphene template, which is capable of boosting the unidirectional growth of nanocrystals.^{39,40}

In contrast to surfactant-capped AuNWs, whose radical growth is fully suppressed by the capping agent,^{25, 33-36} AuNWs obtained here *via* surfactant-free route not only grow in the longitudinal direction but also enlarge radically with adsorbing more newly reduced Au atoms (Figs. S8 and inset of Fig. 3(c)). As a result, the relations of diameters and aspect ratios with the time t are summarized in Fig. S9. Interestingly, both relations of D v.s. t and R v.s. t are mastered by the Avrami theoretical model, indicative of kinetically controlled growth of AuNWs on the graphene template.³² In this step, high-dense stacking faults are observed, which is a common type of planar defects in many nanocrystals, as presented in Fig. 3(c). Its atomic structure reveals stacking faults are gathered in $\langle 111 \rangle$ direction, which is identified by FFT spots streaking along $\langle 111 \rangle$ vector on $\{110\}$ basal planes (Fig. S10).

In addition, the attachment of Au nanoparticles to AuNWs surface suggests the growth has not been completed. They require extra time to fuse nanoparticles, accommodate more adatoms, and heal structural defects. Consequently, it makes Au nanowires smoother, longer, and straighter (Fig. S8(d) and Fig. 3(d)). Moreover, the atomic structure in the selected area at this step discloses Au atoms are closely packed on defect-free

{111} planes along the longitudinal direction, as shown in Fig. 3(e), which is consistent with Au orientations in the early stages.

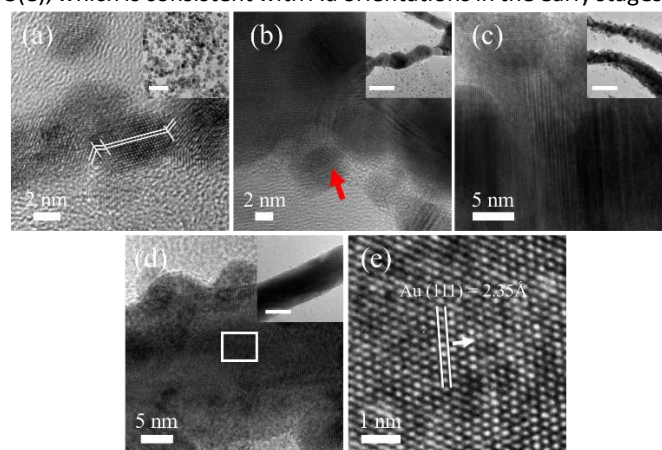


Figure 3. Structural evolution of Au nanowires on graphene template in different timeframes, t . (a) 1 hr (b) 4 hrs (c) 12 hrs and (d) 24 hrs. (e) Atomic structure of the selected area in the white box of (d). Insets in figs. (a)-(d) are the corresponding low magnification images. Scale bars in the insets are 20 nm.

We summarize the growth mechanism of graphene templated AuNWs as a multiple-step strategy (Fig. 4). In short, plasma treatment activates graphene surfaces with defective sites (Fig. 4(a), step 1), which breaks the epitaxial relation between graphene hexagonal lattice and Au nuclei.¹¹ Such defective sites can also function as the anchoring spots for freshly reduced Au clusters due to the enhanced binding energy with Au atoms (Fig. 4(b), step 2). The utilization of ultrasonication at the same time facilitates the symmetry breaking of Au clusters, and triggers OA event at the nano-scale (Fig. 4(c), step 3), which ensures relatively small diameters of final AuNWs.

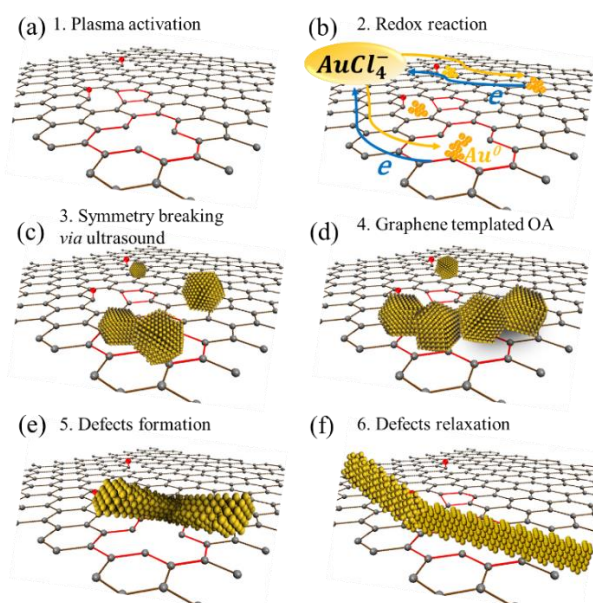


Figure 4. Schematic illustration of the growth mechanism of AuNWs on graphene template. Red balls and sticks represent hydrophilic functional groups and defective graphene sites.

Ultrathin AuNWs formed at this stage show favourable alternating orientations, benefit from graphene's direction. Due to a weak bonding, Au nanoparticles are rotatable on graphene surface, leading to the achievement of graphene templated OA,

from which Au single-crystalline structure tends to form, albeit with structural defects (Fig. 4(d), (e), step 4-5). These two steps guarantee single-crystalline structures of AuNWs. Ultimately, with extra time to diffuse the adatoms and heal planar defects, AuNWs complete the growth ended with smooth surfaces and defect-free structures (Fig. 4(f), step 6). As the counterpart, AuNWs obtained without ultrasonication are derived from synergetic functions of graphene induction and Cl⁻ ions stabilization.^{11,38,41} In short, after Au nanoparticles coalescence, their growth is identical from step 4 to step 6 as shown in Figure 4.

In conclusion, AuNWs are successfully synthesized with graphene template direction via an ultrasonication assisted approach, which readily present two important features—high aspect ratio (up to 5,000) and single-crystalline structure. The high aspect ratio is attributed to the utilization of ultrasound, which breaks the symmetrical growth of Au nanocrystals and promotes the formation of AuNWs at the early stages. Single-crystalline AuNWs are obtained relying on the step by step guidance of graphene template. This research brings new insights to the synthesis of dimension-controllable Au nanocrystals on the graphene support and inspires the development of novel graphene-based nanocomposites.

Acknowledgements

This work was financially supported by the U.S. Department of Defense (fund # 000-16-C-0081). We also thank Dr. Chao Li at the Department of Materials Science and Engineering at UCLA for the analysis and discussion of XRD measurement.

Conflicts of interest

There are no conflicts of interest to declare.

References

- Q. Quan, X. Lin, N. Zhang and Y.-J. Xu, *Nanoscale*, 2017, **9**, 2398–2416
- H. Huang, L. Ma, C. S. Tiwary, Q. Jiang, K. Yin, W. Zhou and P. M. Ajayan, *Small*, 2017, **13**, 1603013.
- Z. Lou, M. Fujitsuka and T. Majima, *J. Phys. Chem. Lett.*, 2017, **8**, 844–849
- X. Li, W. Qi, D. Mei, M. L. Sushko, I. Aksay and J. Liu, *Adv. Mater.*, 2012, **24**, 5136–5141
- N. N. Nguyen, S. B. Jo, S. K. Lee, D. H. Sin, B. Kang, H. H. Kim, H. Lee and K. Cho, *Nano Lett.*, 2015, **15**, 2474–2484
- W. Xin, J.-M. Yang, C. Li, M. S. Goorsky, L. Carlson and I. M. De Rosa, *ACS Appl. Mater. Interfaces*, 2017, **9**, 6246–6254
- Y. Liu, R. Cheng, L. Liao, H. Zhou, J. Bai, G. Liu, L. Liu, Y. Huang and X. Duan, *Nat. Commun.*, 2011, **2**, 579
- H. Moon, D. Kumar, H. Kim, C. Sim, J.-H. Chang, J.-M. Kim, H. Kim and D.-K. Lim, *ACS Nano*, 2015, **9**, 2711–2719
- K. Jasuja and V. Berry, *ACS Nano*, 2009, **3**, 2358–2366
- S. Z. Nergiz, N. Gandra, S. Tadepalli and S. Singamaneni, *ACS Appl. Mater. Interfaces*, 2014, **6**, 16395–16402
- W. Xin, I. M. De Rosa, P. Ye, J. Severino, C. Li, X. Yin, M. S. Goorsky, L. Carlson and J.-M. Yang, *Nanoscale*, 2018, **10**, 2764–2773
- Y. K. Kim, H. K. Na, Y. W. Lee, H. Jang, S. W. Han and D. H. Min, *Chem. Commun.*, 2010, **46**, 3185–3187
- A. N. Sidorov, G. W. Sławiński, A. H. Jayatissa, F. P. Zamborini and G. U. Sumanasekera, *Carbon*, 2012, **50**, 699–705
- A. Hoggard, L. Wang, L. Ma, Y. Fang, G. You, J. Olson, Z. Liu, W. Chang, P. M. Ajayan and S. Link, *ACS Nano*, 2013, **7**, 11209–11217
- M. J. Walsh, S. J. Barrow, W. Tong, A. M. Funston and J. Etheridge, *ACS Nano*, 2015, **9**, 715–724
- M. J. Walsh, W. Tong, H. Katz-Boon, P. Mulvaney, J. Etheridge and A. M. Funston, *Acc. Chem. Res.*, 2017, **50**, 2925–2935
- K. D. Gilroy, H.-C. Peng, X. Yang, A. Ruditskiy, and Y. Xia, *Chem. Commun.* 2017, **53**, 4530–4541
- S. Zhou, D. S. Mesina, M. A. Organt, T. Yang, X. Yang, D. Huo, M. Zhao and Y. Xia, *J. Mater. Chem. C*, 2017, DOI:10.1039/C7TC05625G
- L. M. Chen, C. P. Deming, Y. Peng, P. G. Hu, J. Stofan and S. W. Chen, *Nanoscale*, 2016, **8**, 14565–14572
- M. R. Langille, M. L. Personick, J. Zhang and C. A. Mirkin, *J. Am. Chem. Soc.*, 2012, **134**, 14542–14554
- M. L. Personick, M. R. Langille, J. Zhang and C. A. Mirkin, *Nano Lett.*, 2011, **11**, 3394–3398
- A. Das, S. Pisana, B. Chakraborty, S. Piscanec, S. K. Saha, U. V. Waghmare, K. S. Novoselov, H. R. Krishnamurthy, A. K. Geim, A. C. Ferrari and A. K. Sood, *Nat. Nanotechnol.*, 2008, **3**, 210–215
- Q. Zhang, S. Liu and S. Yu, *J. Mater. Chem.*, 2009, **19**, 191–207
- K.-S. Cho, D. V. Talapin, W. Gaschler and C. B. Murray, *J. Am. Chem. Soc.*, 2005, **127**, 7140–7147
- A. Halder and N. Ravishankar, *Adv. Mater.*, 2007, **19**, 1854–1858
- P. G. Hu, L. M. Chen, X. W. Kang and S. W. Chen, *Acc. Chem. Res.*, 2016, **49**, 2251–2260
- P. G. Hu, L. M. Chen, C. P. Deming, L. W. Bonny, H. W. Lee and S. W. Chen, *Chem. Commun.*, 2016, **52**, 11631–11633
- L. Yu, G. Zhang, C. Yuan and X. W. Lou, *Chem. Commun.*, 2013, **49**, 137–139
- C. Zhu, H.-C. Peng, J. Zeng, J. Liu, Z. Gu and Y. Xia, *J. Am. Chem. Soc.*, 2012, **134**, 20234–20237
- S. Balasubramanian, A. Sheelam, K. Ramanujam and R. Dhamodharan, *ACS Appl. Mater. Interfaces*, 2017, **9**, 28876–28886
- X. Gao, F. Lu, B. Dong, Y. Liu, Y. Gao and L. Zheng, *Chem. Commun.*, 2015, **51**, 843–846
- T. Guo, G. Yu, Y. Zhang, H. Xiang, F. Chang and C.-J. Zhong, *J. Phys. Chem. C*, 2017, **121**, 3108–3116
- Z. Huo, C.-K. Tsung, W. Huang, X. Zhang and P. Yang, *Nano Lett.*, 2008, **8**, 2041–2044
- K. Critchley, B. P. Khanal, M. Ł. Górzny, L. Vigderman, S. D. Evans, E. R. Zubarev and N. A. Kotov, *Adv. Mater.*, 2010, **22**, 2338–2342
- X. Huang, S. Li, S. Wu, Y. Huang, F. Boey, C. L. Gan and H. Zhang, *Adv. Mater.*, 2012, **24**, 979–983
- H. Cui, C. Hong, A. Ying, X. Yang and S. Ren, *ACS Nano*, 2013, **7**, 7805–7811
- J. M. Yuk, M. Jeong, S. Y. Kim, H. K. Seo, J. Kim and J. Y. Lee, *Chem. Commun.*, 2013, **49**, 11479–11481
- L. Pei, K. Mori and M. Adachi, *Langmuir*, 2004, **20**, 7837–7843
- J. L. Xie, C. X. Guo and C. M. Li, *Energy Environ. Sci.*, 2014, **7**, 2559–2579
- H. Wang, H. Yi, X. Chen and X. Wang, *J. Mater. Chem. A*, 2014, **2**, 1165–1173
- W. Xin, J. Severino, I. M. De Rosa, D. Yu, J. McKay, P. Ye, X. Yin, J.-M. Yang, L. Carlson and S. Kodambaka, *Nano Lett.*, 2018, DOI: 10.1021/acs.nanolett.7b05173